CHAPTER IV
RESULTS AND DISCUSSION

4.1 Titanium Oxide Characterization

The silver/silver-chloride (Ag/AgCl) reference electrode was constructed in a metal body to overcome the temperature restriction of 250-300 °C for Teflon which is the material usually used for electrical insulation of high temperature electrodes. Since titanium is well known for its excellent resistance to corrosion, primarily due to a passive oxide layer at the surface, it was chosen for this design to study a passive film on the electrode body. When exposed to air at elevated temperatures, 300 °C or more, a thick oxide film is developed (Broumas *et al.*, 2003). In order to avoid the electrical conductivity between the silver wire and metal electrode body, the titanium tube was oxidized to act as an electrical insulator. The experimental procedure is described in Section 3.2.

The oxide film formed was yellow in color and was observed to evenly coat both the inner and outer surfaces of the titanium tube. A section of the inner surface section of the tube was analyzed using Scaning Electron Microscopy (SEM), Energy Dispersive X-Ray Microanalysis (EDAX) and X-ray Diffraction (XRD). Figure 4.1 shows the surface morphology of titanium oxide as revealed by the SEM technique. It was observed that the titanium oxide film is uniform and of an average crystal size of 1 μm. Figure 4.2 shows the thickness of the oxide layer at the edge of the tube approximately 60 μm. The XRD pattern, shown in Figure 4.3, demonstrates that TiO_2 (rutile phase) was identified as the major composition of oxide film. The EDAX analysis also confirms the presence of a predominant TiO_2 phase. Since there are no other peaks observed from EDAX spectrum, we confirmed that the oxide film composition had no impurity phase. The oxide film produced by this method showed durability in the static system experiments over extended periods.

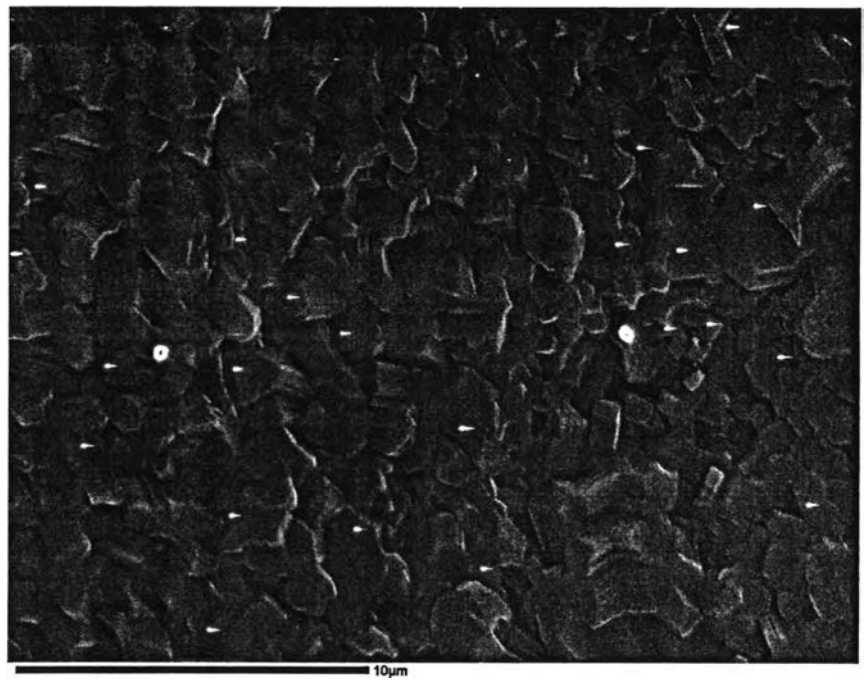

Figure 4.1 Oxidized titanium surface analysis by SEM technique.

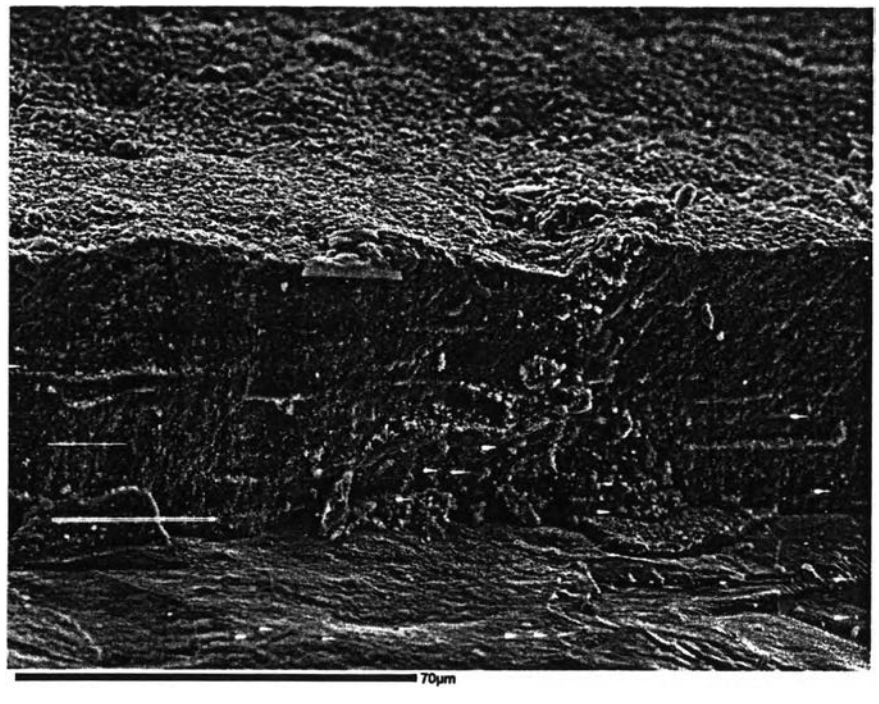

Figure 4.2 Titanium oxide thickness on the titanium tube.

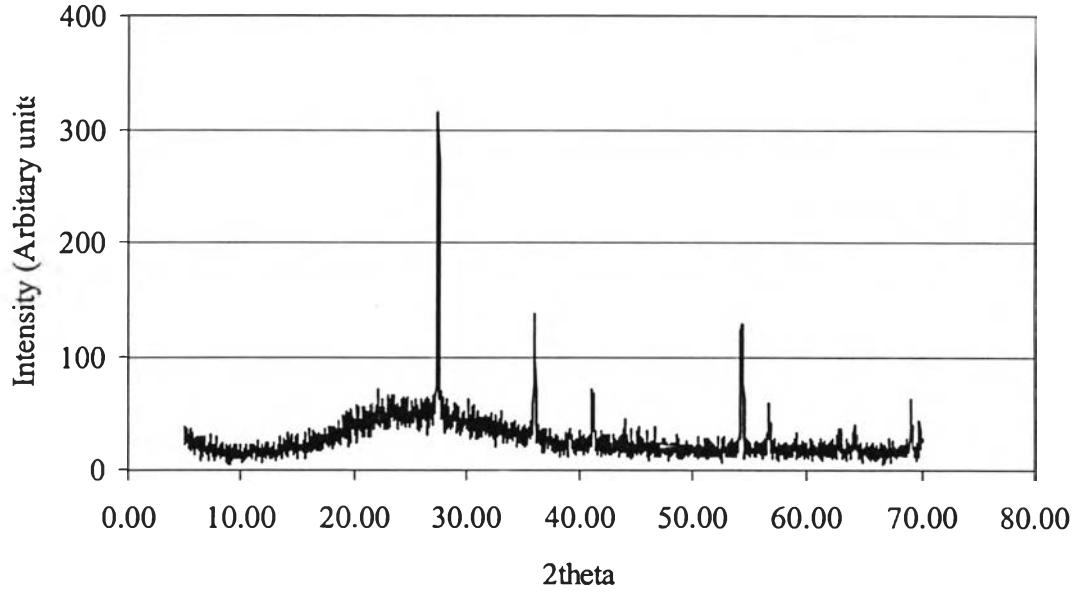

Figure 4.3 XRD pattern of titanium oxide.

4.2 Stability of the Reference Electrode

It was first necessary to demonstrate that the silver/silver-chloride (Ag/AgCl) reference electrode could work reliably at ambient conditions and that its potential was constant over extended periods. The Ag/AgCl reference electrode was verified by measuring its potential against a standard calomel reference electrode (SCE). Filling solutions of 0.1 M, 1 M, 3.5 M and saturated KCl were used to check the electrode's viability. The measured potentials are shown in Table 4.1 and compared to the theoretical values. The measured potential differences are 0.043 ± 0.002 V, -0.005 ± 0.001 V, -0.043 ± 0.001 V and -0.047 ± 0.002 V for filling solution concentrations of 0.1 M, 1 M, 3.5 M and saturated KCl respectively. The results also demonstrate that the electrode potentials were consistent with a reproducibility of ± 0.003 V achievable at room temperature.

Figure 4.4 shows the electrode's potential converted to the SHE scale. The standard calomel reference electrode has a potential +0.241 V versus NHE (Bard *et al.*, 2000). Comparing the experimental data with the theoretically calculated potential of Ag/AgCl reference electrode, a qualitative agreement was attained within ± 0.005 V.

Table 4.1 Silver/silver-chloride (Ag/AgCl) reference electrode potentials versus standard calomel electrode at room temperature

[KCl] (M)	Measured potential (V, vs. SCE)				Theoretical value (V, vs SCE)
	i	2	3	Avg.	
0.1	0.045	0.042	0.042	0.043 ± 0.002	0.047
1	-0.005	-0.006	-0.005	-0.005 ± 0.001	-0.006
3.5	-0.044	-0.042	-0.043	-0.043 ± 0.001	-0.039
Sat.	-0.048	-0.048	0.045	-0.047 ± 0.002	-0.045

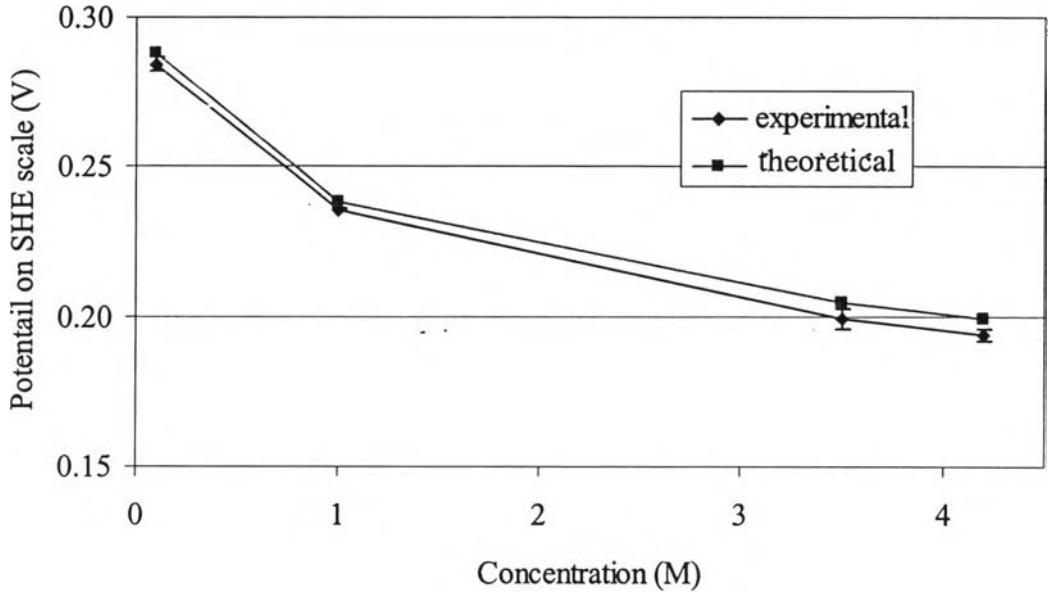

Figure 4.4 Concentration dependence of Ag/AgCl electrode potential at room temperature.

The stabilities over time of the electrode with various fill-solution concentrations are shown in Figures 4.5- 4.8. After a short equilibrating period, the electrode potentials were essentially constant, showing good stability for up to 4 hours. Stable potentials of the electrode within ± 0.005 V of the theoretical values were generally established after 20-40 minutes.

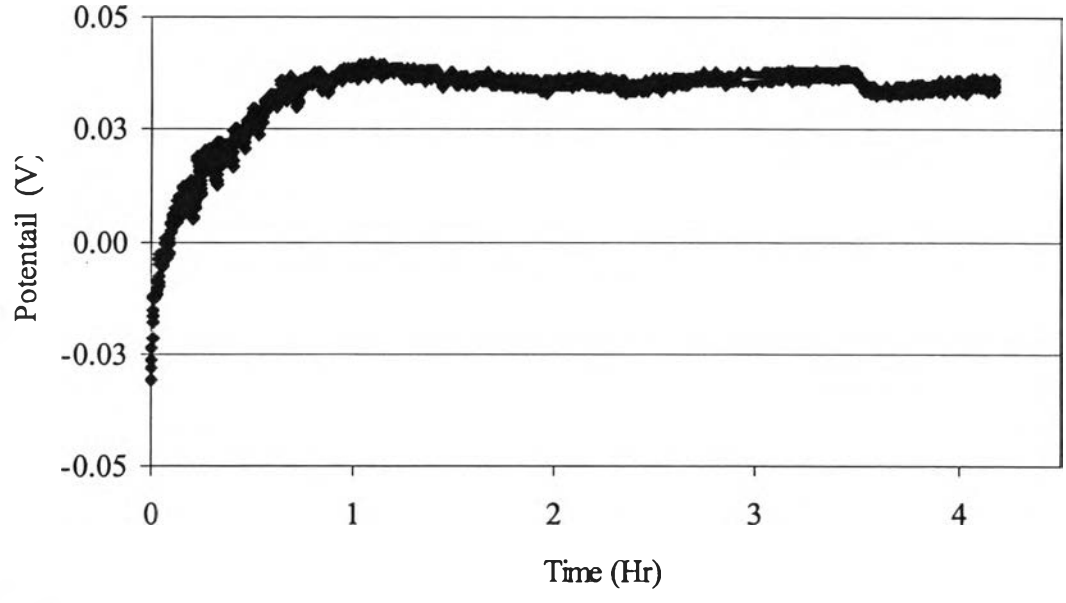

Figure 4.5 Ag/AgCl electrode potential stability at 0.1 M KCl.

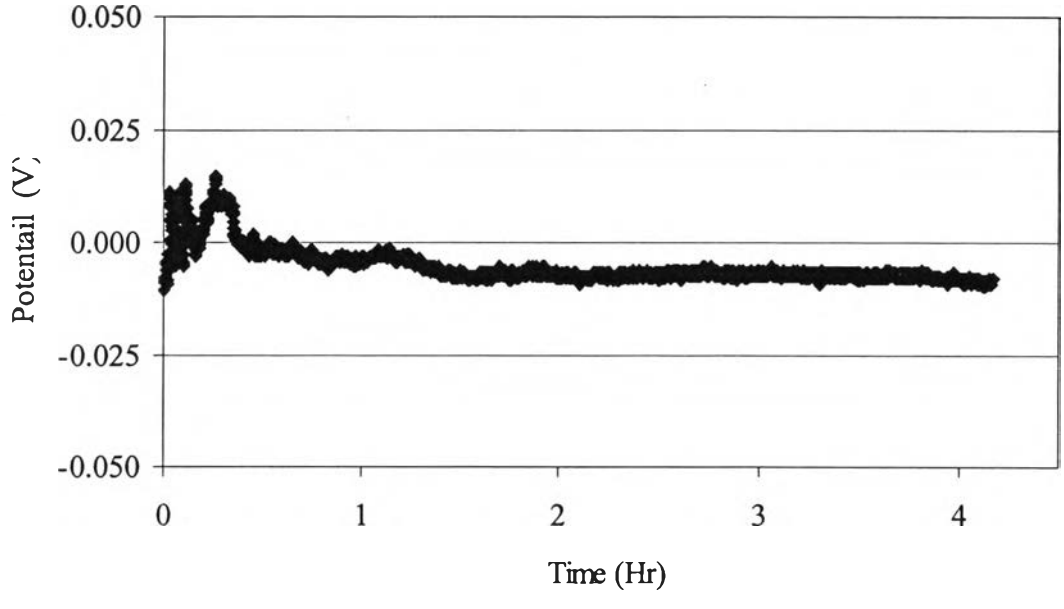

Figure 4.6 Ag/AgCl electrode potential stability at 1 M KCl.

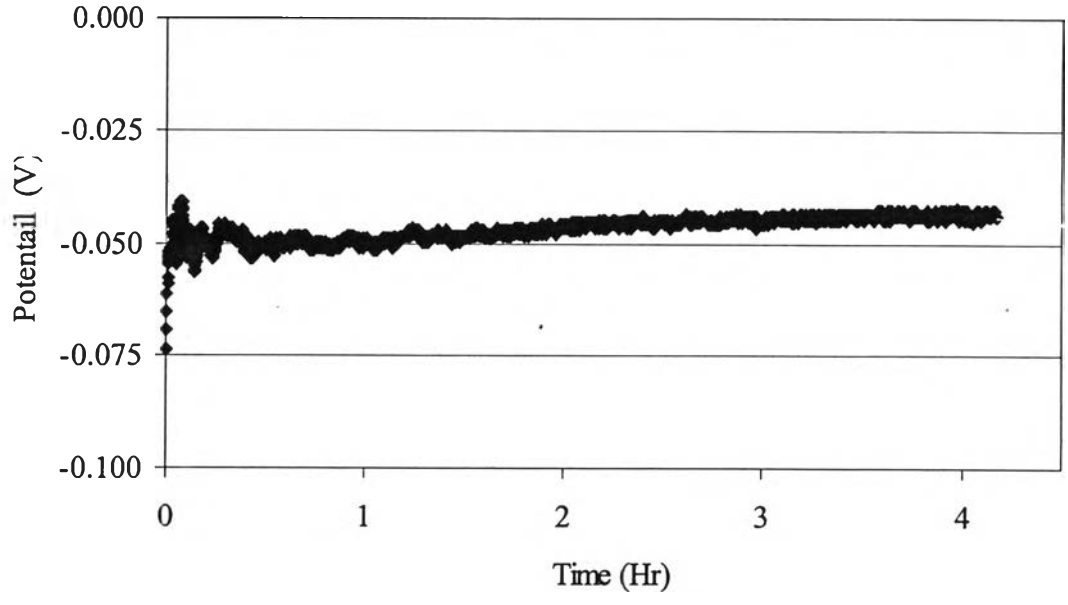

Figure 4.7 Ag/AgCl electrode potential stability at 3.5 M KCl.

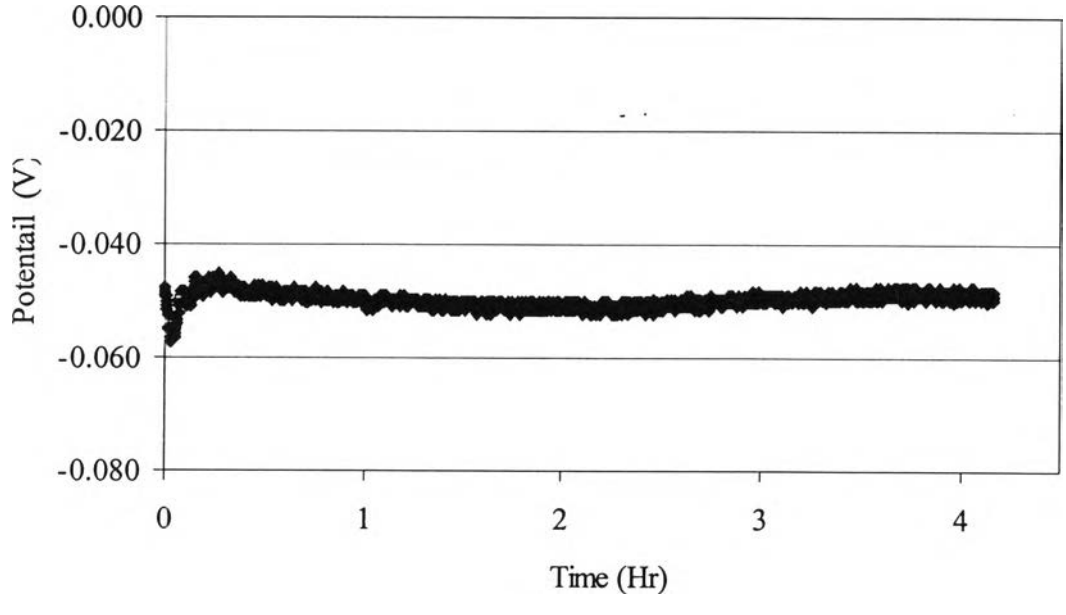

Figure 4.8 Ag/AgCl electrode potential stability at saturated KCl.

Reference electrode potentials can naturally change over time due to the transport and depletion of ions and solvent across the junction. The rate of change is a function of the difference in composition between the sample solution and the filling solution. In this case chloride anions and potassium cations continuously

diffuse out to the test solution in order to complete the measurement circuit. A gradual dilution of the internal solution led to a drift in electrode potential. Therefore, it was recommended that the electrode be checked periodically for accuracy.

The Ag/AgCl, filled with saturated KCl, was continually monitored for one week to test for long-term accuracy. Results show that it can be used for at least a week with a minimal potential drift of 4 mV (Figure 4.9). The filling solution should also be recommended to be replenished as often as possible or as necessary for the required precision.

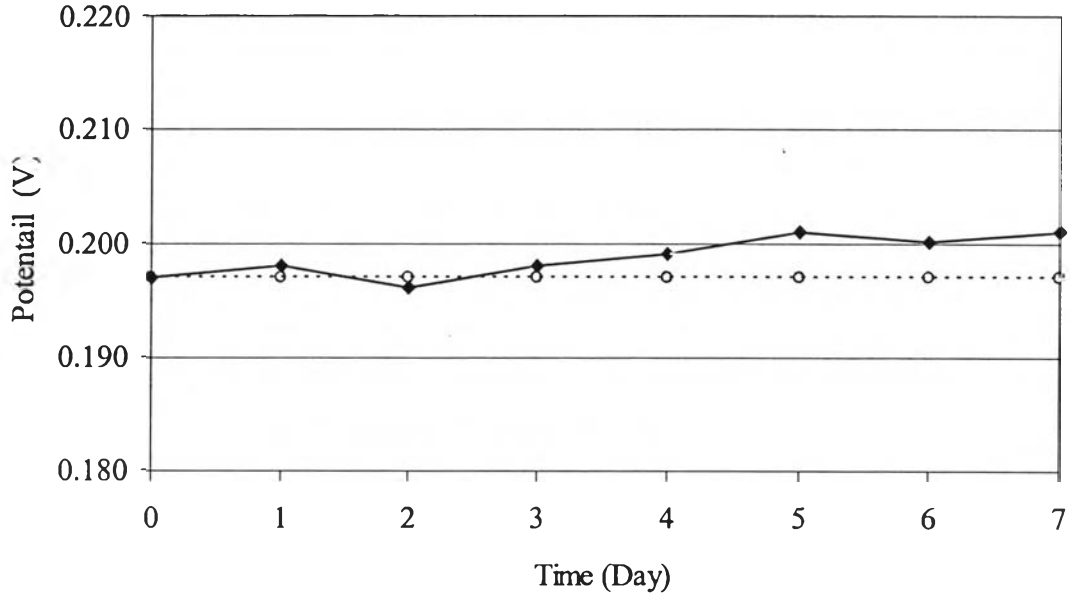

Figure 4.9 Ag/AgCl electrode potential versus time (broken line is the initial electrode potential).

4.3 Temperature Dependence of Electrode Potential

To verify the high temperature electrode performance, the Ag/AgCl electrode was tested by measuring the potential difference against a platinum electrode under high temperature and high pressure conditions. The thermal cell is expressed as:

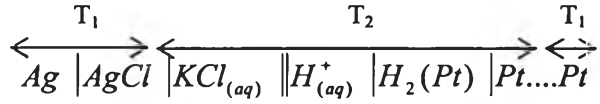

Potential differences between two electrodes were monitored continuously while the autoclave temperature was raised in steps to a maximum temperature of 300 °C. The experimental results at three different KCl fill solution concentrations (0.01 M, 0.1 M and 0.5 M KCl) are plotted in Figure 4.10. By recording the data in ascending and descending directions, the Ag/AgCl electrode showed reproducibility of ±25 mV in the temperature range of 25-300 °C.

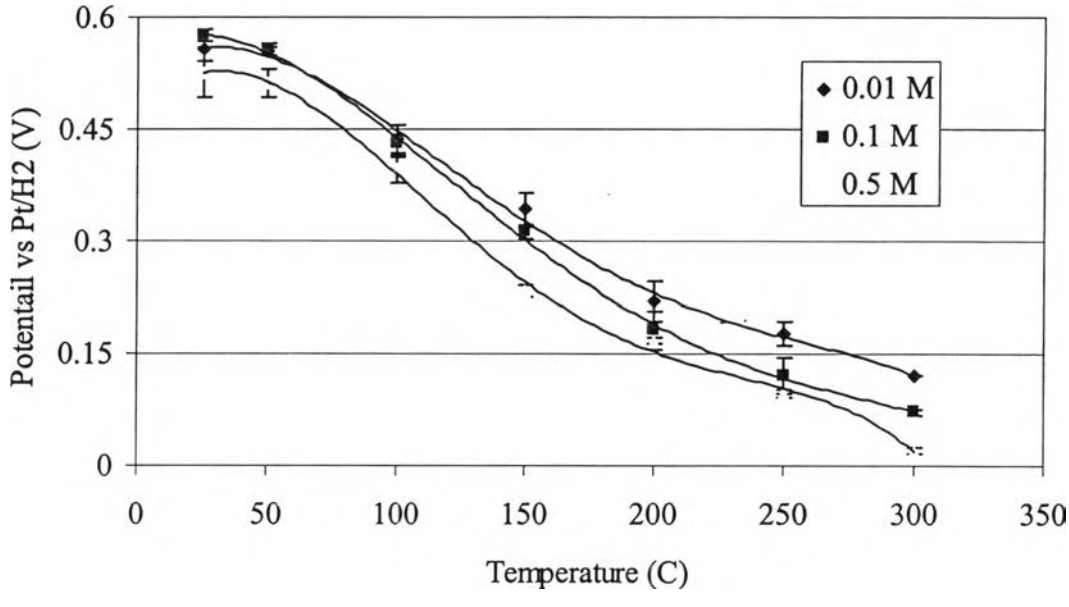

Figure 4.10 Temperature dependence of AgCl reference electrode versus Pt electrode.

The Ag/AgCl electrode potential was checked versus a calomel reference electrode before and after the autoclave testing. Results are shown in Table 4.2. The electrode showed reproducibility by repeating the measured potential before and after a test within ± 30 mV. The KCl filling solution was diluted during the test resulting in an increase in electrode potential after the high temperature test

Table 4.2 Ag/AgCl reference electrode potential versus SCE before and after autoclave testing

KCl Conc. (M)	Trial	Potential (V)		Theoretical value* (V)
		before	after	
0.001	1	0.0809	0.1210	0.0964
	2	0.1056	0.1154	
	3	0.9387	0.9530	
0.1	1	0.0223	0.0599	0.0441
	2	0.0403	0.0622	
	3	0.0411	0.0578	
0.5	1	-0.0246	0.0152	-0.0038
	2	-0.0107	0.0221	

* Theoretical value calculated from Equation 2.3

The Ag/AgCl electrode serves as the working electrode and the platinum wire as reference electrode during the experiment (Figure 3.2). The Ag/AgCl electrode potential on SHE scale is based on the following equation;

$$E_{AgCl}(T) = \Delta E_{meas} + E_{Pt} \tag{4.1}$$

where E_{AgCl} = Ag/AgCl electrode potential on SHE scale at temperature T

E_{Pt} = platinum electrode potential on SHE scale at temperature T

ΔE_{meas} = measured potential difference

In order to relate the Ag/AgCl electrode potential onto the SHE scale the potential of the platinum electrode is required. The reaction occurring on the platinum electrode is the reversible hydrogen reaction;

$$2H^+ + 2e \leftrightarrow H_2 \tag{4.2}$$

The potential of the platinum electrode is given by the Nernst Equation;

$$E_{H^+/H_2} = E^o_{H^+/H_2} \quad \frac{RT}{nF} \ln \frac{P_{H_2}}{a^2_{H^+}} \tag{4.3}$$

where E_{H^+/H_2} = Reversible hydrogen reaction potential on platinum electrode

$E^o_{H^+/H_2}$ = standard potential of Reversible hydrogen reaction potential on platinum electrode at temperature 298 °K

a_{H^+} = chloride ion activity

P_{H_2} = partial pressure of hydrogen gas

$\because E^o_{H^+/H_2} = 0$ and $pH = \log a_{H^+}$ Equation 4.2 yield to;

$$E_{H^+/H_2} = \frac{2.303RT}{nF} \log \frac{P_{H_2}}{a^2_{H^+}} \tag{4.4}$$

$$E_{Pt} = \frac{2.303RT}{nF} (\log P_{H_2} + 2pH) \tag{4.5}$$

The potential of platinum electrode is fixed by purging the test solution with a known concentration of dissolved hydrogen at a known pH. Since the autoclave was purged with pure hydrogen gas for several hours prior to the experiment, it was assumed that hydrogen was present at a pressure of 1 atm in the static system. The potential of the platinum electrode is defined as:

$$E_{Pt}(T) = \frac{2.303RT}{F}(pH) \tag{4.6}$$

The ionization product of water is necessary in order to calculate the pH of the solution at each temperature. The Marshall and Franck correlation was employed to estimate the dissociation equilibrium constant of water (K_w) as a function of temperature (Marshall and Frank, 1981).

Pure water undergoes autopyrolysis to yield equal numbers of hydrogen and hydroxide ions;

$$H_2O \leftrightarrow H^+ + OH \tag{4.7}$$

The equilibrium constant is expressed as;

$$K_w = [H^+][OH^-] = 10^{-14} \text{ at } 25\ ^\circ C \tag{4.8}$$

The Marshall and Frank correlation for log K_w as a function of temperature is;

$$\log K_w = A + BT + CT^2 + DT^3 + ET^4 \tag{4.9}$$

values of the parameters are;

A = -14.9378

B = 4.2404×10^{-2}

C = -2.1025×10^{-4}

D = 6.2203×10^{-7}

E = -8.7383×10^{-10}

The pH of pure water from 25-300 °C is shown in Table 4.3. The pH of water decreased with temperature resulting in a decrease of the platinum electrode potential with temperature as shown in Fig 4.11.

Table 4.3 Test solution pH as a function of temperature

Temperature (°C)	log Kw	[H+]	pH
25	-14.000	1.000E-07	7.0000
50	-13.271	2.315E-07	6.6355
100	-12.265	7.369E-07	6.1326
150	-11.651	1.495E-06	5.8254
200	-11.289	2.267E-06	5.6445
250	-11.172	2.595E-06	5.5858
300	-11.422	1.944E-06	5.7112

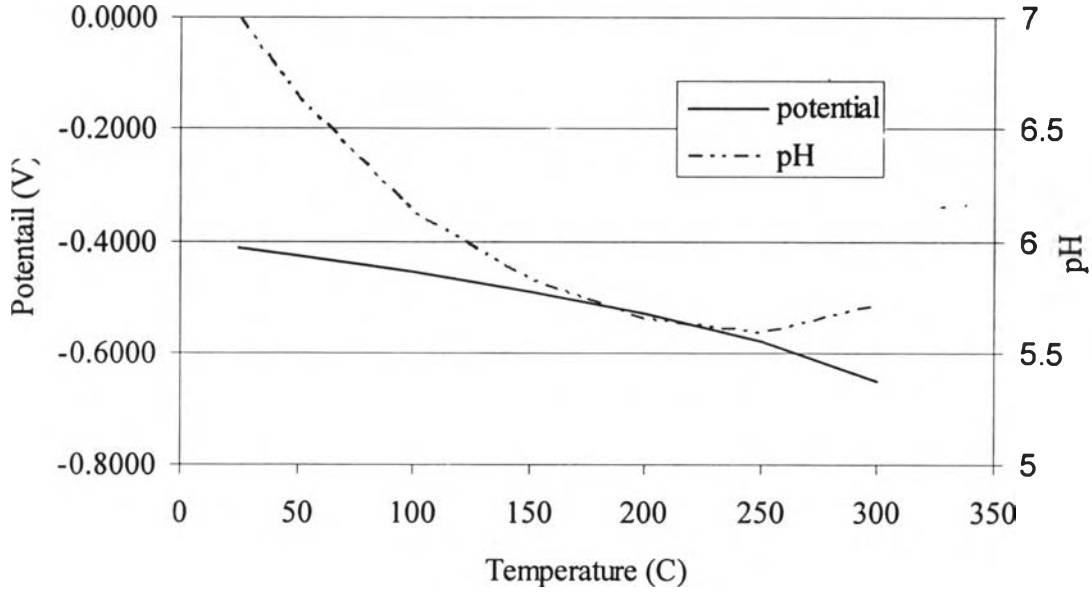

Figure 4.11 Pt electrode potential as a function of temperature and pH of solution.

Once the Pt electrode potential is known, the Ag/AgCl electrode potential versus the Pt electrode was converted onto the SHE scale by Equation 4.1. Results are shown in Figure 4.12.

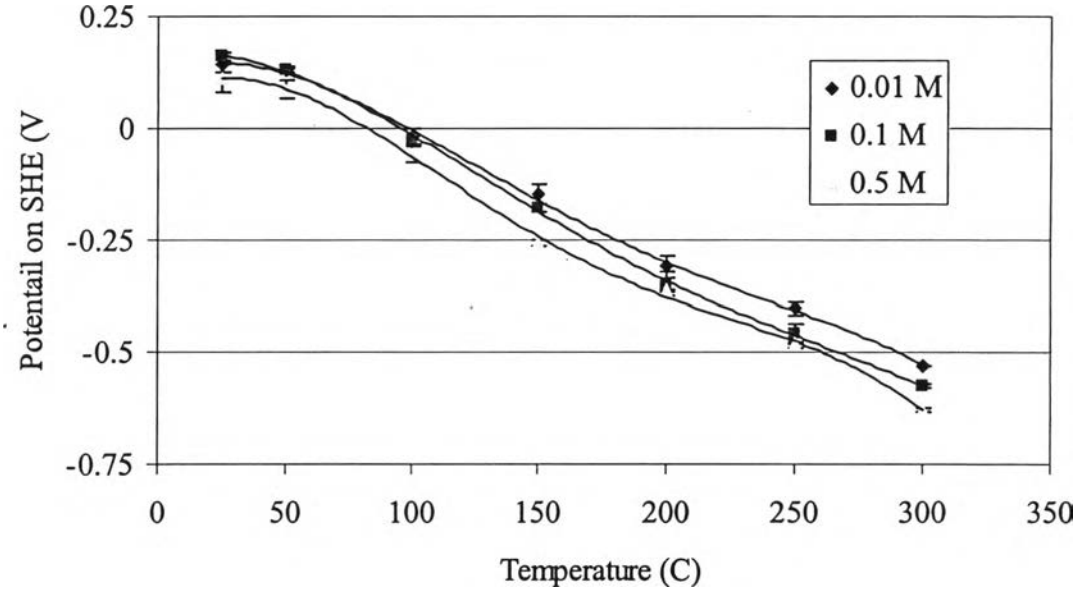

Figure 4.12 Ag/AgCl electrode potential on SHE scale as a function of temperature.

The Nernstain potentials of the Ag/AgCl reaction at elevated temperatures were calculated in order to compare the measured Ag/AgCl electrode potential with the theoretical value. Due to the instability of the AgCl layer at high temperature, the cooling system was designed to maintain the AgCl at a low temperature, ideally below 70 °C. where AgCl is known to quickly dissolve. The cooling system used cooling water at approximately 5 °C flowing through a cross fitting as shown in the electrode configuration diagram (Figure 3.1). With a maximum cooling flow rate of 0.13 liter/hour, the AgCl could be maintained at room temperature for operating temperatures up to 100 °C.

Hence, the electrolyte in which AgCl was placed was slightly heated due to the limitation of the cooling efficiency. It was assumed that the temperature of the fill solution at the Ag/AgCl element was equal to the tube surface temperature above the cross. The temperature at this position was recorded by a surface thermocouple at each step change of temperature during the experiment.

The theoretical Ag/AgCl electrode potentials were calculated from Equation 2.3 with the activity coefficients at elevated temperatures shown in Figure 2.2. The observed tube surface temperature above the cross and the corresponding Ag/AgCl

electrode potentials are given in Table 4.4. It can be seen that the Ag/AgCl electrode potential increases with temperature.

Table 4.4 Temperature dependence of Ag/AgCl electrode potential

Temperature (°C)		Electrode potential at KCl conconcentration (V)		
Operating	Above the cross	0.01 M	0.1 M	0.5 M
25	25.0	0.3404	0.2881	0.2402
50	25.0	0.3404	0.2881	0.2402
100	25.0	0.3404	0.2881	0.2402
150	26.3	0.3444	0.2890	0.2513
200	31.1	0.3464	0.2901	0.2517
250	37.5	0.3490	0.2916	0.2524
300	45.0	0.3521	0.2932	0.2532

Comparing the measured and calculated Ag/Ag Cl electrode potentials, the deviation from theory, E^*, is shown in Figure 4.13. It was observed that a greater deviation of the Ag/AgCl electrode potential occurred with increasing temperature. In order to validate the accuracy of the Ag/AgCl reference electrode, a correction factor needed to be formulated to compensate for this potential deviation. A potential correction was empirically modelled in which the contributions of potentials possibly generated in the system were considered. The liquid junction potential (LJP), thermal liquid junction potential (TLJP) as well as all of potentials generated due to temperture effects need to be accounted for in correcting the measured potential to the theoretical value.

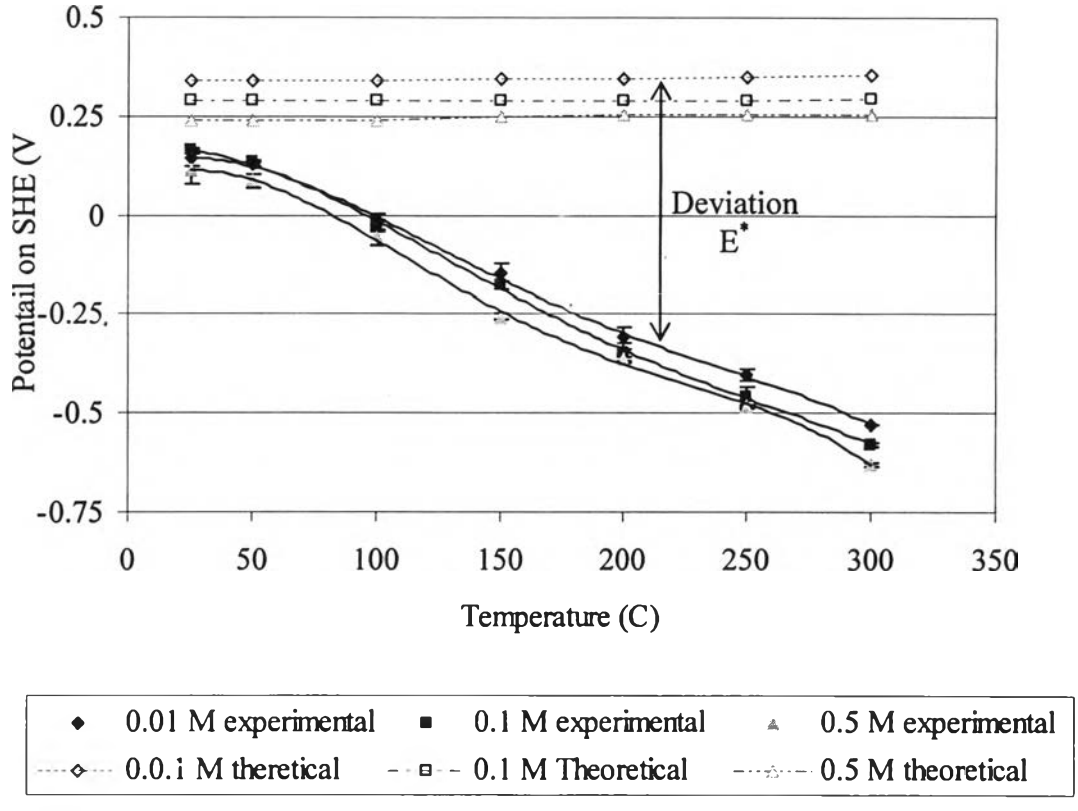

Figure 4.13 Comparison of measured and calculated Ag/AgCl electrode potential as a function of temperature.

4.4 Electrode Potential Modelling

4.4.1 Potential Correlation

It can be seen in Figure 4.13 that the Ag/AgCl electrode potentials deviated from their theoretical values. The potential correlation is a tool for correcting the observed potential to its theoretical potential by accounting for all interfering potentials in the experiments.

The correlation was modeled assuming that the measured potential is the sum of all potentials generated in system. Therefore, all of the thermal diffusion phenomena were taken into account and determined as a function of temperature. The first of which is a liquid junction potential (LJP), generated due to the concentration gradient of filling solution across the plug. Also, the temperature

gradient along the length of the electrode body is generated and produces a thermal liquid junction potential (TLJP).

One reaction that may occur on the oxidized titanium tube is

$$TiO_{2(s)} + 4H^{+}_{(aq)} + 4e \leftrightarrow Ti_{(s)} + 2H_2 0_{(liq)} \qquad (4.10)$$

As stated above, to measure the electrochemical potential there must be an electrolyte bridge to complete the circuit between the two electrodes. At room temperature, Cl^- anions diffuse out through the bottom plug to create the electrolyte bridge. There has been considerable debate in the literature regarding oxygen vacancy versus titanium interstitial models for self-diffusion in rutile TiO_2 (Handersan, 1999). Therefore, at higher temperatures, species self-diffusion in titanium/titanium oxide could be considered as another current pathway, similar to zirconium metal.

Various methods have been used to study oxygen self-diffusion in oxides such as the resonance capture technique (Derry *et al.*, 1971). However, increased rates of diffusion in Ti interstitials have been pointed out by use of nuclear reaction analysis (NRA) (Erickson and Rogers, 1988). There has also been numerous studies if diffusion in rutile TiO_2 that do not rely on only oxygen or titanium diffusion. For example, Sasaki *et al.*, suggested that the oxygen diffusion in TiO_2 is linked to cooperative diffusion of impurity cations.

The idea of two current path ways during high temperature measurement are depicted in Figure 4.14. Figure 4.14 a) shows the exchange of K^+ cations and Cl^- anions with the test solution through the capillary (threads) to provide the connection path. The measured potential is simply expressed as;

$$\Delta E_{meas} = E_{AgCl} \quad E_{Pt} + LJP + TLJP \qquad (4.11)$$

where E_{mea} = measured potential difference between the Ag/AgCl electrode and the platinum electrode

E_{AgCl} = theoretical Ag/AgCl electrode potential

E_{Pt} = potential of H^+/H_2 reaction at Pt electrode versus SHE

LJP = liquid junction potential

$TLJP$ = thermal liquid junction potential

In the case the bottom of the tube is plugged, and no electrolyte bridge is installed (Figure 4.14 b). At high temperatures, the potential difference between the platinum electrode and Ag/AgCl electrode could be measured due to oxygen diffusion through the Ti/TiO_2. The correlation generates a measured potential which equation is given by the following

$$\Delta E_{meas} = E_{AgCl} \quad E_{Pt} + TLJP + 2E_{TiO_2} \tag{4.11}$$

where ΔE_{meas} = measured potential difference (V)

E_{AgCl} = theoretically calculated Ag/AgCl reference electrode (V)

E_{Pt} = platinum electrode potential

$TLJP$ = thermal liquid junction potential

E_{TiO_2} = titanium dioxide reaction potential

Notice that the potential of the TiO_2 reaction is doubled to account for the reaction occurring on both the outer and inner surfaces of the titanium tube.

Once parallel electrolyte bridges exist, one could be more dominant than the other. The following equation is purposed to estimate the potential deviation of Ag/AgCl electrode, E^*, from its theoretical value. The term δ is added to compensate for the parallel paths.

$$\Delta E_{meas} = E_{AgCl} \quad E_{Pt} + E^* \tag{4.12}$$

E^* = fraction through capillary + fraction diffused

$$E^* = \delta(LJP + TLJP) + (1 \quad \delta)(2E_{TiO_2} + TLJP) \tag{4.13}$$

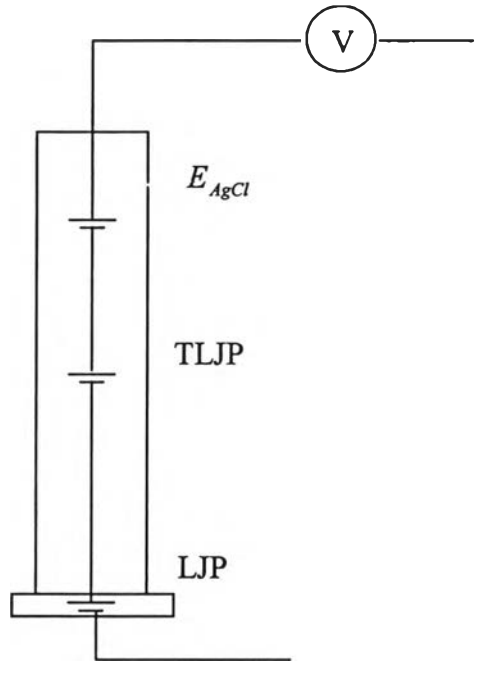

a)

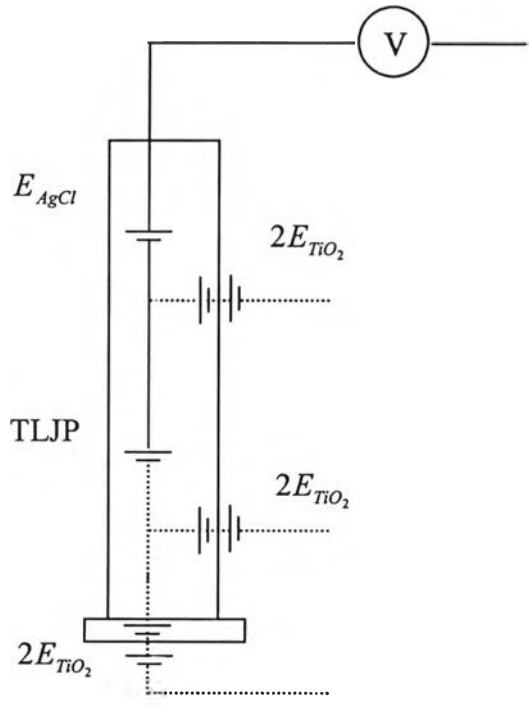

b)

Figure 4.14 The idea of two current pathways at Ag/AgCl electrode during potential measurement; a) Low temperature conditions and b) High temperature conditions and the bottom end is plugged.

Where ΔE_{meas} = measured potential difference between the Ag/AgCl electrode and the platinum electrode

E_{AgCl} = theoretical Ag/AgCl electrode potential

E_{Pt} = potential of H^+/H_2 reaction at Pt electrode versus SHE

LJP = liquid junction potential

$TLJP$ = thermal liquid junction potential

E^* = Correction potential

E_{TiO_2} = TiO_2 reaction potential

δ = compensating term for parallel electrolyte conduction paths

4.4.1.1 Liquid Junction Potential

The magnitude of the liquid junction potential (LJP) depends on ions present in the system, together with their relative concentration, valencies, mobilities and temperature across the junction. Potassium chloride was chosen as the filling solution in this work with the purpose of minimizing the liquid junction potential. The mobilities of potassium ion and chloride ion are nearly equal, therefore; both of the ions move at the same rate across the junction, no charge accumulates on either side of the solution.

The comparison of experimental and theoretical values of Ag/AgCl electrode potential from the bench tests are in excellent agreement, thus, it was deducted that there was no liquid junction potential effect at room temperature for this electrode configuration. However, liquid junction potential is a temperature dependent phenomenon and can not be ignored in high temperature conditions. Neglecting the influence of LJP at room temperature, Table 4.5 summarizes the liquid junction potential calculaled by Equations 2.4 and 2.5 from the operating temperature range of 50-300 °C. The LJP values are slightly different among the three concentrations of KCl.

Table 4.5 Temperature and KCl concentration dependence of liquid junction potential

Temperature (°C)	Liquid junction potential (V)		
	0.01 M	0.1 M	0.5 M
50	-0.0110	-0.0122	-0.0130
100	-0.0127	-0.0141	-0.0150
150	-0.0144	-0.0160	-0.0171
200	-0.0161	-0.0179	-0.0191
250	-0.0178	-0.0197	-0.0211
300	-0.0195	-0.0216	-0.0231

4.4.1.2 Thermal liquid junction potential

The thermal liquid junction potential (TLJP) calculated using Equation 2.7 are tabulated in Table 4.6 as a function of temperature. These values are in reasonable agreement with the estimate of ± 0.3 mV K^{-1} given by De Benthune *et al.*, 1959. As the temperature differences become greater, the TLJP is found to increase rapidly in the positive direction.

Table 4.6 Temperature and KCl concentration dependence of thermal liquid junction potential

Temperature (°C)	Thermal liquid junction potential (V)		
	0.01 M	0.1 M	0.5 M
25	0.0000	0.0000	0.0000
50	0.0036	0.0038	0.0035
100	0.0193	0.0189	0.0192
150	0.0510	0.0458	0.0476
200	0.1038	0.0864	0.0902
250	0.1833	0.1428	0.1482
300	0.2949	0.2168	0.2231

4.4.1.3 Titanium Oxide Reaction

The titanium oxide reaction potential can be calculated according to electrochemistry principles through the change in free energy of reaction (ΔG_r), as it is related to the change in the energy of a charge as it passes through the potential difference (E_r) at the metal/solution interface. The correlation is defined as;

$$\Delta G_r = nFE_r \tag{4.14}$$

where ΔG_r = reaction free energy at temperature T (J/mol)

E_r = reversible potential difference across the interface (V)

n = number of electrons transferred in the reaction

F = Faraday number (96485 C/mol)

The reaction free energy can be estimated through the standard free energy of formation of each component at temperature T from the fundamental relationship;

$$\Delta G_r = \sum G^o_{products}(T) \quad \sum G^o_{reactants}(T) \tag{4.15}$$

where G^o = standard free energy of formation of each component at temperature T (Jol/mol)

The standard free energies of formation of components, those which are required for the evaluation of ΔG_r in Equation 4.10, are listed in Table 4.7. The calculated ΔG_r as a function of temperature is plotted in Figure 4.15 and the corresponding calculated E_{TiO_2} at each test temperature is shown in Table 4.8.

Table 4.7 Standard free energy of formation of titanium dioxide reaction components (Barin and Knacke, 1973; Barner and Scheuerman, 1987)

Temperature (K)	G^{o} (kcal mol^{-1})			
	TiO_2*	H^+	Ti	H_2O**
298	-229.39	0	-2.184	-73.305
300	-229.41	0	-2.198	-73.339
400	-230.83	0	-3.026	-75.292
500	-232.61	0	-4.013	-77.695
600	-234.71	0	-5.131	-80.474

* Rutile phase Titanium dioxide

** Liquid phase

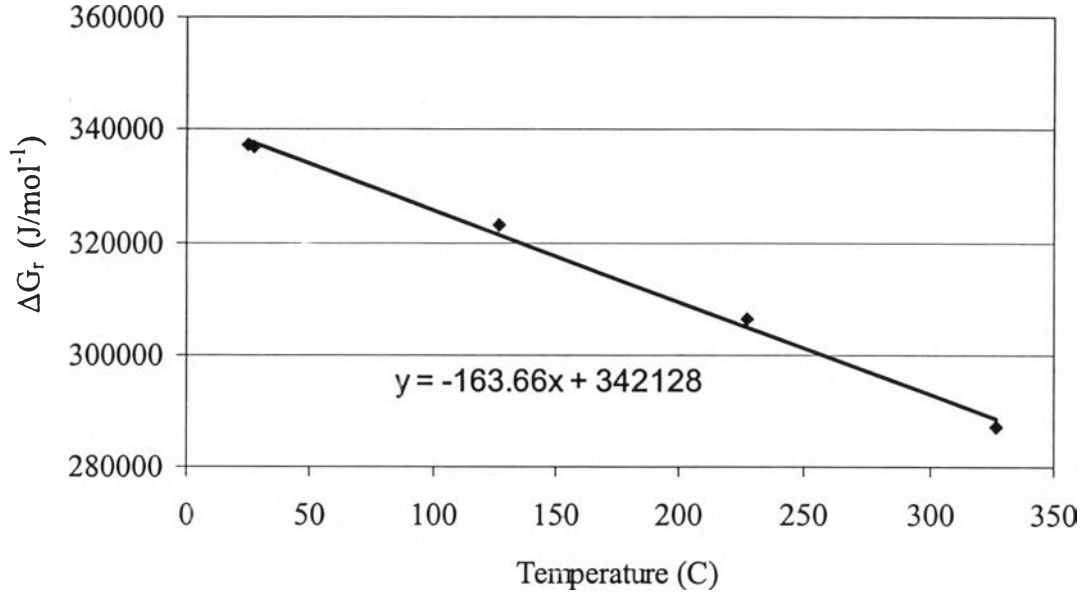

Figure 4.15 Titanium dioxide reaction free energy as a function of temperature.

Table 4.8 Calculated titanium dioxide reaction potential , E_{TiO_2} ,as a function of temperature

Temperature (°C)	E (V)
25	-0.8765
50	-0.8665
100	-0.8465
150	-0.8265
200	-0.8065
250	-0.7865
300	-0.7665

Substituting the data and the known parameters, LJP, TLJP and E_{TiO_2}, into Equation 4.12 and 4.13, the compensating term, δ, was determined and given in Table 4.9 as a function of KCl concentration and temperature. It can be seen that the compensating term decreases with temperature for all KCl concentrations. According to Equation 4.13, the capillary fraction, diffusing out through the threads, is interpreted to be less significant at higher temperature. On the other hand, the weighting term, 1-δ, for the self-diffusion though the Ti/TiO_2 is more dominant due to the acceleration of species movement at high temperatures.

4.4.2 Model Application

The measured potential of any electrode of interest versus the Ag/AgCl reference electrode can be related to the SHE scale by the correlation;

$$\Delta E_{SHE} = \Delta E_{meas} + E_{AgCl} + E^{*} \qquad (4.16)$$

where ΔE_{SHE} = potential of electrode of interest on SHE scale (V)

ΔE_{meas} = measured potential difference (V)

Table 4.9 Compensating term for parallel electrolyte conduction paths

Temperature (°C)	δ (at KCl concentration)		
	0.01 M	0.1 M	0.5 M
25	0.8877	0.9293	0.9266
50	0.8817	0.9169	0.9163
100	0.7826	0.8066	0.8196
150	0.6778	0.7012	0.6710
200	0.5339	0.5504	0.5692
250	0.4099	0.4269	0.4441
300	0.2356	0.2929	0.2830

E_{AgCl} = theoretically calculated Ag/AgCl reference electrode (V)

$E^{\bullet}$ = correction potential

Substituting $E^{\bullet}$ from Equation 4.12, then Equation 4.15 yields,

$$\Delta E_{SHE} = \Delta E_{meas} + E_{AgCl} + 2E_{TiO_2} + \delta(LJP \quad 2E_{TiO_2}) + TLJP \qquad (4.17)$$

E_{TiO_2} = titanium dioxide reaction potential (V)

LJP = Liquid junction potential (V)

$TLJP$ = Thermal liquid junction potential (V)

δ = compensating term

To validate the accuracy of the correction terms, the potential of a carbon steel coupon was measured using the Ag/AgCl electrode as a reference. The corrected carbon steel potentials were compared for the measured potentials versus the Ag/AgCl reference electrode with electrolyte 0.1 and 0.5 M KCl. The measured potential differences, the correction potentials and the corrected potential of carbon steel are shown in Table 4.10. Results show that the empirical correction gives corrected potentials that are in good agreement, within 17 mV of each other.

Compared to data by other researchers, the corrected carbon steel potential is well within the range of the carbon steel ECP, -700 mV to -400 mV, observed at 142 °C in a flowing system (Shao, UNB Nuclear; Private communication, 2004).

Table 4.10 Measured and corrected carbon steel corrosion potential against Ag/AgCl reference electrode (KCl filling solution)

T (°C)	25	50	100	150	200	250	300
0.1 M							
ΔE_{meas}	-0.1846	-0.2055	-0.2571	-0.3429	-0.3940	-0.2742	-0.1619
E_{AgCl}	0.2881	0.2881	0.2881	0.2890	0.2901	0.2916	0.2932
E_{TiO2}	-0.8765	-0.8665	-0.8465	-0.8265	-0.8065	-0.7865	-0.7665
LJP	0.0000	-0.0122	-0.0141	-0.0160	-0.0179	0.0197	-0.0216
TLJP	0.0000	0.0038	0.0189	0.0458	0.0864	0.1428	0.2168
δ	0.9293	0.9169	0.8066	0.7012	0.5504	0.4269	0.2929
ΔE^{*}_{SHE}	-0.0205	-0.0688	-0.2889	-0.5132	-0.7525	-0.7499	-0.7422
0.5 M							
E_{meas}	-0.1403	-0.1708	-0.2171	-0.2729	-0.3940	-0.2822	-0.1179
E_{AgCl}	0.2402	0.2402	0.2402	0.2513	0.2517	0.2524	0.2532
E_{TiO2}	-0.8765	-0.8665	-0.8465	-0.8265	-0.8065	0.7865	-0.7665
LJP	0.0000	-0.0130	-0.0150	-0.0171	-0.0191	-0.0211	-0.0231
TLJP	0.0000	0.0035	0.0192	0.0476	0.0902	0.1482	0.2231
δ	0.9266	0.9163	0.8196	0.6710	0.5695	0.4441	0.2830
ΔE^{**}_{SHE}	-0.0287	-0.0840	-0.2754	-0.5293	-0.7574	-0.7654	-0.7473
Error	0.0082	0.0153	0.0134	0.0161	0.0049	0.0155	0.0050

Note: Error = $|\Delta E^{*}_{SHE} \quad \Delta E^{**}_{SHE}|$